LIFE PREDICTION FOR RANDOM LOAD FATIGUE BASED ON THE GROWTH BEHAVIOR OF MICROCRACKS

H. H. Heitmann, H. Vehoff and P. Neumann

Max-Planck-Institut fuer Eisenforschung, 4000 Duesseldorf, Federal Republic of Germany

ABSTRACT

A crack initiation life prediction scheme is proposed by integrating a growth law for micro-cracks. The growth of small cracks is described by the effective cyclic J-integral, Z. From this procedure a new damage parameter, Z_d, is defined which contains the plastic strain range, the stress range, and the mean stress. The latter two improve the prediction in the high cycle regime. In order to carry out this type of life prediction a couple of specimens are required to obtain cyclic stress strain curves from incremental step tests and about 10 specimens to obtain an SN-curve in terms of the Z_d parameter. No crack growth data are required because of the intimate connection between life and crack growth law. Experimental results on mean stress effects and on random loading are compared with the predictions using Z_d as well as the Smith-parameter.

KEYWORDS

Fatigue, crack initiation, small cracks, crack propagation, cyclic J-integral, random loading, Masing behavior, damage accumulation, life prediction, steels.

INTRODUCTION

Many proposals have been made for predicting the fatigue life under variable amplitude loading on the basis of constant amplitude loading data. Most of these approaches are based on phenomenologically defined damage parameters, which are supposed to determine the increment of damage done to the material within each cycle (Miner's law). In such approaches the physical nature of the fatigue damage as well as of the damage parameters remain unspecified. In the present paper it was tried to avoid both drawbacks by defining the fatigue damage as the maximum crack length present. Life predictions can then be made by integrating the appropriate general crack growth law. Studies of this kind were done previously (Kaisand and Mowbray, 1979, Tanaka, Hoshide, and Maekawa 1982) but were not applied to random loading. On the other hand this study is limited to life predictions on smooth specimens only.

EXPERIMENTAL

Two low alloy structural steels, StE 47, StE 70, and one quench and tempered steel 38NiCrMoV 7 3 (AISI 4340) were used. The latter one was heat treated to two different yield strengths of 740 and 1100 MPa. Smooth tensile specimens with a diameter, D, of 6 or 8 mm and a gauge length of 2D were machined with the specimen axis perpendicular to the rolling direction. The surface of the gauge length was polished mechanically.

The specimens were fatigued in a computer controlled hydraulic closed-loop testing system. The compliance was measured on-line with high precision, such that the plastic strain amplitude could be determined with an accuracy of better than 10^{-5}. The length of the surface cracks was measured optically.

The random load tests were performed by repeating a quasi-random total strain pattern with about 1000 reversal points. The strains at the reversal points were distributed according to a clipped distribution function $\rho = 1/\varepsilon^{*}\exp(-\varepsilon/\varepsilon^{*})$. ε^{*} was chosen in such a way that the damage due to small and large plastic strain ranges was about equal.

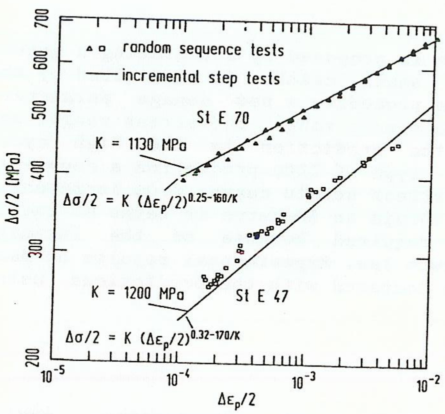

Fig. 1. Stress range versus strain range of closed hystereses loops during random loading tests and incremental step tests.

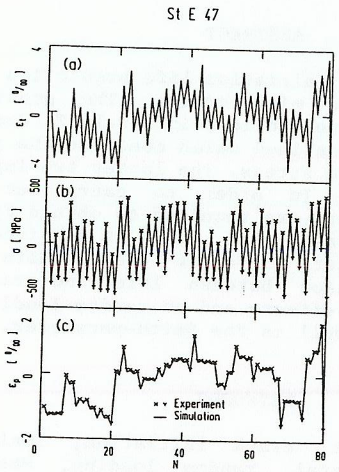

Fig. 2. Predicted and measured plastic strain ranges during random total strain tests.

CYCLIC STRESS STRAIN BEHAVIOR.

Usually the loading history is given in terms of the reversal values of either the stress or the total strain. On the other hand the plastic strain amplitude is a very important quantity for estimating the fatigue damage as is obvious from the fairly general validity of Coffin-Manson's law (Manson 1953, Coffin 1954). Therefore, as a first step a prediction of the plastic strains from the given stress or total strain history must be performed. This was done by using the well-known Masing-model of cyclic stress strain behavior, which is characterized by the existence of a universal function, the so-called cyclic stress strain curve, which uniquely relates ranges (between reversal points) of stress and plastic strain as long as both are increasing monotonically (Masing 1926). For general loading histories the cyclic memory effect is assumed which enforces rain-flow counting of the closed hystereses loops (Martin, Topper, and Sinclair 1970).

The three steels used show a Masing-type behavior to a reasonable degree of accuracy. The main problem is cyclic softening which is not included in the Masing-model. Because of deviations from the ideal Masing behavior cyclic stress strain curves depend on the exact way how they are measured. Those which were obtained by incremental step tests (Landgraf, Morrow, and Endo 1969) were found to be most similar to the relation between stress ranges and plastic strain ranges during random loading. Both are compared in fig. 1. If strong cyclic softening is observed, however, incremental step test and random loading must have comparable maximum loads to obtain a reasonable agreement. Obviously the cyclic stress strain curve can be approximated by a power-law

$$\Delta\varepsilon_p = C_1\,\Delta\sigma^n \qquad (1)$$

The two material parameters C_1 and n can be measured by an incremental step test with a single specimen. Figure 2 shows an example of the prediction of the peak values of the plastic strain calculated from the peak values of the total strain. It is obvious that there is a good correlation with the measured values. In the following we shall use therefore only cyclic stress strain curves obtained from incremental step tests.

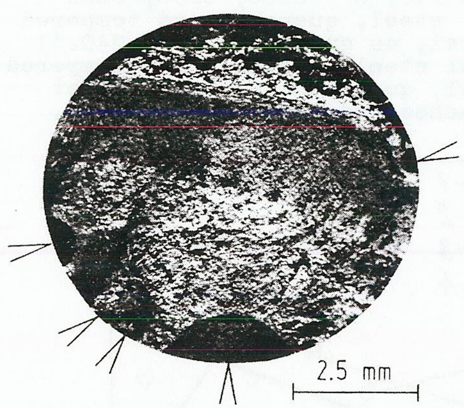

Fig. 3. Semi-circular surface cracks marked by heat tinting on a fracture surface.

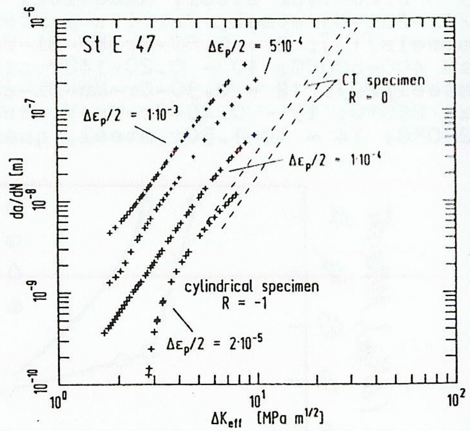

Fig. 4. Growth rate of small cracks as a function of the nominal effective stress range.

THE GROWTH OF MICRO CRACKS.

During random loading microcracks are obtained as soon as the first high peak load is applied. Thus more than 90% of the technical crack initiation life ($a \leq 1$ mm) is spent by growth of these microcracks. They originate at surface inclusions (ZrS, or more complex inclusions) which are about 30 μm in diamater. Initially the cracks are of comparable size. Depending on the load level, there are many crack nuclei (fig. 3), which grow independently as long as their lengths are smaller than their mutual distances. This was found by observing the growth of many individual cracks with the help of an optical microscope. The cracks have a well defined almost semi-circular shape with a depth to width ratio of 0.89/2, which agrees with finite element calculations of the local stress intensity along the front of thumbnail surface cracks (Raju and Newman 1979).

As shown in fig. 4 the growth behavior of such short cracks cannot be described in terms of ΔK_{eff}-values. The usual fast growth of small cracks compared to long cracks is observed, because linear fracture mechanics is not applicable to this case of small cracks embedded in a fully plastified specimen. For such a case in uni-directional loading the J-integral is the appropriate loading parameter. Since J-integral arguments can be transferred to cycling loading of Masing-type materials (Lamba 1975, Wuethrich 1982) we follow the arguments of Dowling 1977, who estimated the J-values for short surface cracks. The cyclic J-integral, which we shall call Z following Wuethrich, 1982, in order to distinguish it from the uni-directional J-integral, is composed of a plastic, W_p, and an elastic, W_e, part according to

$$Z_{eff} = a\,(f_1 \cdot W_{e\ eff} + f_2 \cdot W_p) \qquad (2)$$

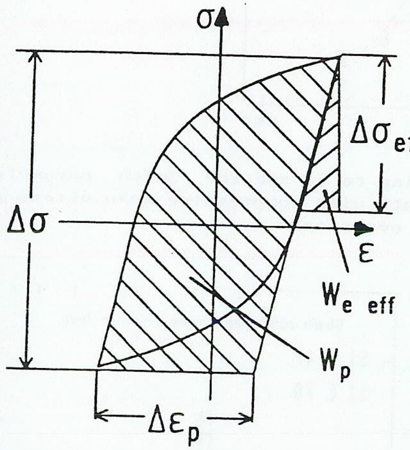

Fig. 5. Definition of the elastic and plastic contributions to the effective cyclic J-integral, Z_{eff}.

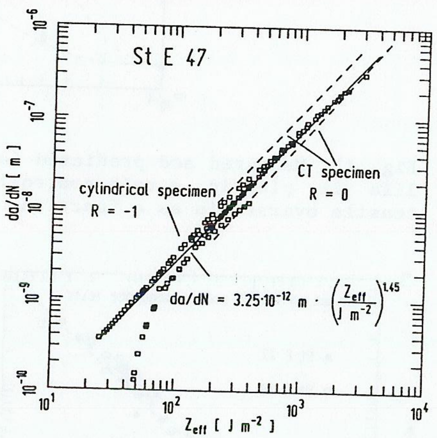

Fig. 6. Growth rate of small cracks as a function of the effective cyclic J-integral Z_{eff}.

With more accurate solutions than those available to Dowling we obtained the following values for the numerical coefficients f_1 and f_2: $f_1 = 2.9$, $f_2 = 2.5$. The definition of W_p and W_e in terms of the hysterese loop, which coincides in Masing type materials with the doubled cyclic strain curve, are given in fig. 5. Thus the loop shape is given by (1) and we obtain

$$W_{e\ eff} = \frac{\Delta\sigma_{eff}^2}{2E} \qquad W_p = \frac{n}{n+1}\,\Delta\sigma\,\Delta\varepsilon_p = \frac{C_1 n}{n+1}\,\Delta\sigma^{n+1} \qquad (3)$$

Crack closure is assumed for the elastic part, W_e, only and not for the plastic part, W_p. The effective stress range due to closure, σ_{eff}, is obtained according to

$$\Delta\sigma_{eff} = \Delta\sigma\ 3.72\ (3 - R)^{-1.74} \qquad R = \frac{\sigma_{min}}{\sigma_{max}} \qquad (4)$$

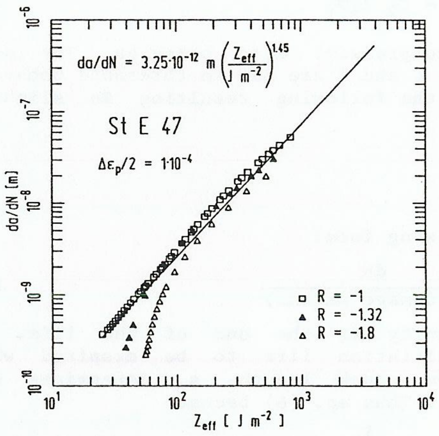

Fig. 7. Crack growth rate of small cracks as a function of the effective cyclic J-integral Z_{eff} for three compressive mean stresses.

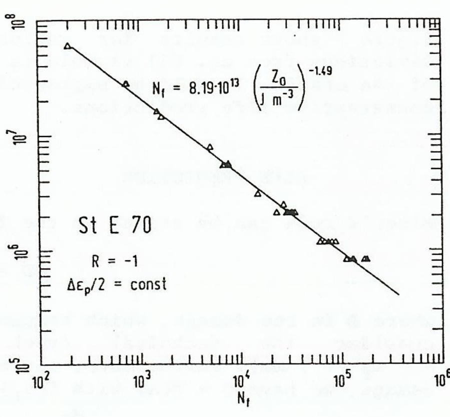

Fig. 8. The technical crack initiation life (a ≤ 1 mm) as a function of the damage parameter Z_d obtained from constant plastic strain range tests.

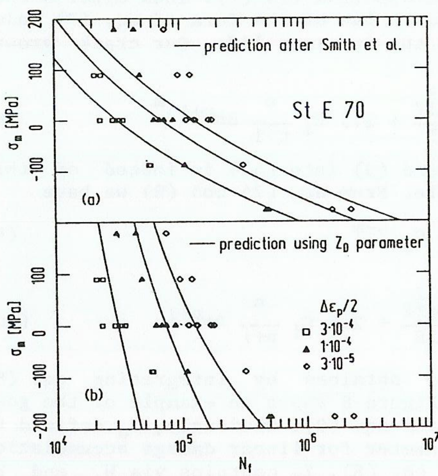

Fig. 9. Cycles to failure as a function of mean stress in constant plastic strain tests. Predictions acoording to Smith et al. and Z_d.

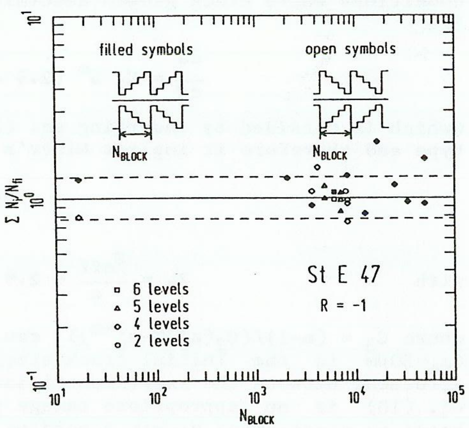

Fig. 10. Calculated damage values at failure for tests with sawtooth loading as a function of the number of cycles within the blocks.

This eq. reproduces Schijve's equation for aluminium (Schijve 1981) for $R > -1$ and extends it to compressive mean stresses without yielding negative values for $R \leq -1$. Figure 6 shows the crack growth data as a function of Z_{eff}. Obviously the data from short as well as long cracks fall on a common line in this double logarithmic plot indicating a power-law dependence of da/dN on Z_{eff}.

$$\frac{da}{dN} = C_2 \, Z_{eff}^{m} \tag{5}$$

Figure 7 shows results for various compressive mean stresses. The only deviations from eq. (5) visible in fig. 6 and 7 are due to threshold behaviour of the cracks. It will be neglected in the following resulting in slightly conservative life predictions.

LIFE PREDICTION

Miner's rule can be stated in the following form:

$$dD = \frac{dN}{N_f(\text{damage param.})} \tag{6}$$

where D is the damage, which becomes unity at the end of the life. We consider the technical crack initiation life to be exspired when $a = a_f$ (= 1 mm). Furthermore, since the crack length, a, determines the damage, we have $D = f(a)$ with $f(a_f) = 1$. Thus eq. (6) becomes

$$\frac{da}{dN} = \frac{1}{df/da \; N_f(\text{damage param.})} \tag{7}$$

The essential point of the form of eq. (7) is, that the crack length dependent part can be separated multiplicatively from the part which depends on the damage parameter. Then eq. (6) follows from eq. (7). Thus Miner's rule is obviously equivalent to a crack growth law of the form of eq. (7) under conditions where crack growth determines the specimen life. Our crack growth law

$$\frac{da}{dN} = C_2 \, a^m \left(2.9 \frac{\Delta\sigma_{eff}^2}{2E} + 2.5 \, C_1 \frac{n}{n+1} \Delta\sigma^{n+1}\right)^m \tag{8}$$

(which is obtained by inserting eq. (2) and (3) into (5)) is indeed of this type and therefore it implies Miner's rule. From eq. (7) and (8) we have

$$N_f = C_3 \, Z_d^{-m} \tag{9}$$

with

$$Z_d = \frac{Z_{eff}}{a} = 2.9 \frac{\Delta\sigma_{eff}^2}{2E} + 2.5 \, C_1 \frac{n}{n+1} \Delta\sigma^{n+1} \tag{10}$$

where $C_3 = (m-1)/(C_2(a_f^{1-m} - a_o^{1-m}))$ can be obtained by integrating eq. (8) (a_o=30µm is the initial crack size). Figure 8 shows an example of the good agreement between the experimental data and eq. (9). Obviously, Z_d defined by eq. (10) is an appropriate damage parameter for linear damage accumulation based on micro-crack growth according to eq. (8). Z_d contains via W_e and W_p both the stress range as well as the plastic strain range. Both terms are necessary in an appropriate damage parameter: The plastic strain term implies Coffin-Manson's law at low cycle fatigue conditions. The stress term makes Z_d a valid damage parameter in the high cycle range, where Coffin-Manson's law breaks down. Note that no adjustable parameters were used at all and eq. (10) was derived - without any further assumptions - from a crack growth law (8) which in turn was derived from fairly well justified fracture mechanics considerations.

Many experiments were performed to test the validity of this prediction

method in block loading tests with mean stresses, which are notoriously difficult to predict (Nowack et al. 1978)). Figure 9 shows the influence of mean stress on the life in tests with constant plastic strain amplitudes together with predictions according to the Smith-parameter (Smith et al. 1970) and according to Z_d. Obviously Z_d works better. Figure 10 shows some results from tests with large abrupt changes in the plastic strain amplitude

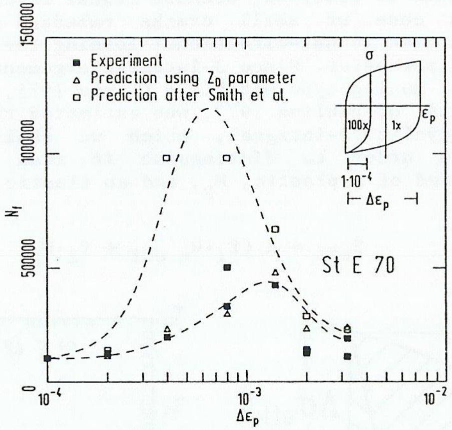

Fig. 11. Measured and predicted (according to Z_d and the Smith parameter) life in plastic strain controlled tests with compressive mean stress and tensile overstrain as a function of the overstrain.

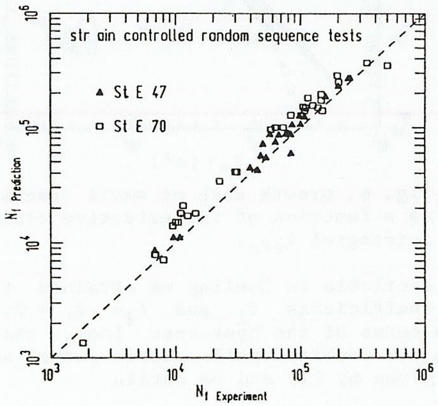

Fig. 12. Comparison of predicted and measured technical crack initiation life for random total strain tests.

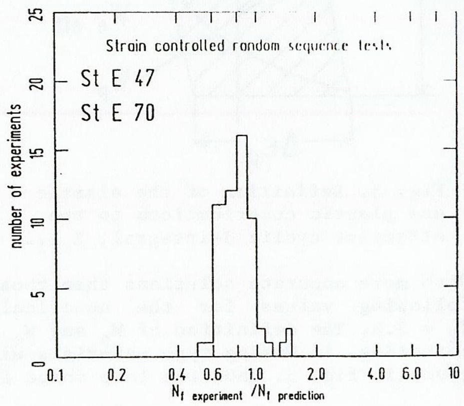

Fig. 13. Distribution function of the ratio between predicted and measured fatigue life in fig. 12.

in both directions (increasing and decreasing). The plastic strain amplitude varied between $2 \cdot 10^{-5}$ and 10^{-3}. The calculated damage at failure has a scatter of about 25% independent of the direction of the amplitude changes indicating that retardation or acceleration effects do not interfere with the prediction. Figure 11 shows the life in bi-harmonic tests with compressive mean strain and repeated tensile overstrains as a function of the amount of overstrain. The Z_d prediction agrees with the data, the Smith-paramater prediction is less accurate.

Figure 12 shows the predictions for random load experiments with an analysis of the scatter in fig. 13. The accuracy of the prediction is of the order of 30% and is slightly non-conservative.

CONCLUSIONS

A short guide-line is given how to proceed in order to make predictions of the technical crack initiation life based on Z_d.

1. An incremental step test with one specimen yields C_1 and n in eq. (1). If there is strong cyclic softening, several tests with different maximum loads must be performed. This provides all the necessary data to calculate Z_d from $\Delta\sigma$ and σ_{mean} according to eq. (10).

2. Constant Z_d fatigue tests (constant $\Delta\varepsilon_p$ tests are sufficient in most cases) with 10 to 20 specimens yield C_3 and m in eq. (9) allowing standard damage accumulation calculations using (6) with (9) i.e. $dD = dN/(C_3 Z_d^{-m})$.

Note: No crack growth measurements need to be performed because of the intimate connection between life and crack growth (eq. (5) and (9)).

ACKNOWLEDGEMENT

Financial support from the Bundesministerium fuer Forschung und Technologie, Bonn, under contract no. 03 S 101 0 is gratefully acknowledged.

REFERENCES

Coffin, L.F. (1954). Transaction of the ASME, 76, 931.
Dowling, N.E. (1977). In: "Cyclic Stress-Strain and Plastic Deformation Aspects of Fatigue Crack Growth", ASTM STP 637, 97.
Kaisand, L.R. and D.F. Mowbray (1979). J. Test. Eval., 7, 270.
Lamba, H.S. (1975). Engng. Fract. Mech., 7, 693.
Landgraf, R.W., J.D. Morrow, and T. Endo (1969). J. Mater. Science, 4, 176.
Lankford, J. and F.N. Kusenberger (1973). Met. Trans., 4, 553.
Manson, S.S. (1953). NASA Techn. Note 2933.
Martin, J.F., T.H. Topper, and G.M. Sinclair (1970). Mater. Research, 11, 23.
Masing, G. (1926). In: "Proceedings of the Second International Congress of Applied Mechanics", Zuerich, 332.
Nowack, H., D. Hanschmann, and K.-H. Trautmann (1978). Fortschritts-berichte der VDI Zeitschriften, 18, 57.
Raju, I.S. and J.C. Newman (1979). Engng. Fract. Mech., 11, 817.
Schijve, J. (1981). Engng. Fract. Mech., 14, 461.
Smith, K.N., P. Watson, and T.H. Topper (1970). J. Mater. Science, 5, 767.
Tanaka, K., T. Hoshide, and O. Maekawa (1960). Engng. Fract. Mech., 16, 207.
Wuethrich, C. (1982). Int. J. Fract., 20, R35.